CrossMark

ORIGINAL ARTICLE

Correlations between dopamine transporter density measured by ^{123}I-FP-CIT SPECT and regional gray matter volume in Parkinson's disease

Tomoko Maekawa[1,2] · **Noriko Sato**[1] · **Miho Ota**[3] · **Atsuhiko Sugiyama**[1] · **Daichi Sone**[1] · **Mikako Enokizono**[1] · **Yukio Kimura**[1] · **Youhei Mukai**[4] · **Miho Murata**[4] · **Harumasa Takano**[5] · **Etsuko Imabayashi**[6] · **Hiroshi Matsuda**[6] · **Akira Kunimatsu**[2] · **Osamu Abe**[2]

Abstract

Purpose Parkinson's disease (PD) is caused by a selective degeneration of dopamine neurons. The relationship between dopamine transporter (DAT) density and gray matter volume has been unclear. Here we investigated the voxelwise correlation between gray matter volume and DAT binding measured by ^{123}I-N-ω-fluoropropyl-2β-carboxymethoxy-3β-(4-iodophenyl)nortropane (^{123}I-FP-CIT) single-photon emission computed tomography (SPECT; DaTscan™ imaging) in PD.

Materials and methods Thirty-one male patients with PD were examined with MRI and DaTscan. To measure nigrostriatal dopaminergic degeneration in PD, the specific binding ratio (SBR) of the striatum was obtained by DaTscan.

Voxel-based morphometry (VBM) of 3D T1-weighted images was used to evaluate the relationships between the regional gray matter volume and the SBR in the striatum.

Results There were significant positive correlations between the SBR and the gray matter volume in the right pulvinar and posterior middle temporal gyrus and a trend level in the left pulvinar, all of which are associated with the second visual pathway.

Conclusion The nigrostriatal dopaminergic degeneration might affect the secondary visual pathway, leading to visual dysfunctions in PD.

Keywords Parkinson's disease · ^{123}I-FP-CIT · Dopamine transporter · Voxel-based morphometry · Secondary visual pathway

✉ Noriko Sato
snoriko@ncnp.go.jp

1 Department of Radiology, National Center of Neurology and Psychiatry, 4-1-1 Ogawa-Higashi, Kodaira, Tokyo 187-8551, Japan

2 Department of Radiology, Graduate School of Medicine and Faculty of Medicine, The University of Tokyo, 7-3-1 Hongo, Bunkyo-ku, Tokyo 113-8655, Japan

3 Department of Mental Disorder Research, National Institute of Neuroscience, National Center of Neurology and Psychiatry, 4-1-1 Ogawa-Higashi, Kodaira, Tokyo 187-8551, Japan

4 Department of Neurology, National Center of Neurology and Psychiatry, 4-1-1 Ogawa-Higashi, Kodaira, Tokyo 187-8551, Japan

5 Department of Psychiatry, National Center of Neurology and Psychiatry, 4-1-1 Ogawa-Higashi, Kodaira, Tokyo 187-8551, Japan

6 Integrative Brain Imaging Center, National Center of Neurology and Psychiatry, 4-1-1 Ogawa-Higashi, Kodaira, Tokyo 187-8551, Japan

Introduction

Parkinson's disease (PD) is a chronic progressive neurodegenerative disorder characterized by motor symptoms such as tremor at rest, rigidity, bradykinesia and postural instability, consequently affecting the quality of life [1]. Neuroimaging studies have contributed to our understanding of the pathophysiology and diagnosis of PD (see review [2]). Single-photon emission computed tomography (SPECT) imaging of dopamine transporter (DAT) is a well-established diagnostic approach to detect nigrostriatal dopaminergic neurodegeneration in parkinsonian syndromes (PS) [2–4]. ^{123}I-N-ω-fluoropropyl-2β-carboxymethoxy-3β-(4-iodophenyl)nortropane (^{123}I-FP-CIT) is the most common radiotracer in clinical studies and shows high sensitivity and specificity for differentiating essential tremor from degenerative PS [4, 5].

🌱 Springer

Voxel-based morphometry (VBM) is an imaging analysis technique that evaluates subtle brain morphologic changes by using high-resolution three-dimensional (3D) T1-weghted magnetic resonance imaging (MRI) data. VBM has been widely used in neuropsychiatric and neurodegenerative disorder research. Many VBM studies have also been reported in PD [6–11], for example, to assess the regional gray matter atrophy of bilateral medial temporal lobes and basal ganglia in comparisons with healthy controls. Several studies reported that non-motor symptoms such as cognitive dysfunction in PD were related to widespread cortical atrophy.

Given that dopaminergic loss is the cardinal sign of neurodegeneration in PD, followed by structural and functional changes in gray matter, the relationship between gray matter volume and DAT density could be important in the pathophysiology of PD. By means of [^{18}F] fluorodeoxyglucose positron emission tomography (FDG PET), PD-related cognitive patterns, which are mainly located in the frontal and parietal association cortex, have been identified, directly covarying with cognitive measures of executive, memory and visuospatial functions [12, 13]. Previous study reports brain perfusion correlates of cognitive and nigrostriatal functions in PD and shows a relevant role of the parietal lobes and posterior cingulate in executive functions in PD [14]. However, the extent to which the severity of dopaminergic striatal denervation is associated with impaired cortical perfusion/metabolism and gray matter volume is still uncertain.

Only one study has evaluated the gray matter changes in association with nigrostriatal dopaminergic degeneration in PD patients by PET using ^{18}F-fluoropropyl-carbomethoxyiodophenylnortropane (^{18}F-FP-CIT) [15]. We conducted the present study to investigate the voxelwise correlation of gray matter volume with DAT density measured by ^{123}I-FP-CIT instead of ^{18}F-FP-CIT in patients with PD.

Materials and methods

Patients

The study population was 31 male PD patients [age range 44–84 years, 67.8 ± 10.8 years (mean ± SD)] who underwent both ^{123}I-FP-CIT and MRI within 3 months using the same SPECT and magnetic resonance (MR) scanners. The clinical diagnoses were made by expert neurologists, and standard diagnoses of PD were made according to the United Kingdom Parkinson's Disease Society Brain Bank Clinical Diagnostic Criteria (steps one and two) [16]. The severity of their Parkinsonism was estimated using the Hoehn and Yahr scale (HY) [17, 18]. This retrospective study received the approval of the institutional review board of our hospital with a waiver of the need for the patients' informed consent.

^{123}I-FP-CIT SPECT data acquisition and analysis

The patient was injected with 167 MBq of ^{123}I-FP-CIT. At 180 min after the intravenous injection, projection data were slowly acquired using SPECT/computed tomography (CT) equipment (Symbia T6, Siemens; Erlangen, Germany) with low- to medium-energy and general-purpose collimators, a 128 × 128 image matrix, zoom factor 1.45, 210 s per cycle and 45 views × 8 cycles. The system resolution was 9 mm full width at half-maximum (FWHM) at a rotating radius of 13 cm. The patient was carefully positioned in the gamma camera in a special head holder that allowed a minimal rotational distance with the orbitomeatal axis in a transverse plane to avoid reorientation during reconstruction.

Image data reconstruction was performed using the 3D ordered-subset expectation maximization method using two subsets and 18 iterations with CT attenuation correction. Scatter collection was not performed. Before the intravenous injection of ^{123}I-FP-CIT, high-quality CT scans for attenuation correction and fusion images were obtained using the same SPECT/CT equipment. The scanning parameters were held constant in the helical scanning mode: 1.0-s gantry rotation time, 130 kVp, 150–240 mAs, 0.5:1 beam pitch, 3-mm table feed per gantry rotation and 6 × 0.5-mm detector configuration. The images were reconstructed at 3-mm thickness with filtered back projection, a display field of view of 25 cm and a reconstruction matrix size of 512 × 512.

We used the present quantifying method already released as DaTView® software (Nihon Medi-Physics, Tokyo). The DaTView technique, which is based on a method developed by Tossici-Bolt et al. [19], is a measurement technique without anatomic standardization that uses a bilateral whole striatal volume of interest (VOI) and the whole brain VOI except for the striatal regions as a reference. We assessed the mean SBR values of the bilateral sides.

MRI data acquisition and processing

All patients underwent MR imaging using a 3-T system (Verio, Siemens Medical Systems, Erlangen, Germany). High-spatial-resolution, 3D T1-weighted images were used for the morphometric study. Anatomical image data sets were acquired with a standard T1-weighted high-resolution anatomic scan of magnetization-prepared rapid gradient echo (MPRAGE) sequence in the sagittal plane: repetition time/echo time/inversion time, 1800/2.26/800 ms; matrix, 288 × 320; field of view 25 × 25 cm; effective section thickness, 0.8 mm with no interslice gap, 224 continuous sagittal slices; number of excitations, 1.

Table 1 Demographic and clinical characteristics of the 31 male patients with Parkinson's disease

	Mean ± SD
Age (years)	67.8 ± 10.8
Onset age (years)	59.6 ± 12.0
Disease duration (months)	93.6 ± 75.2
L-Dopa equivalent dose (mg)	523.4 ± 420.7
	Range
Hoehn and Yahr scale	1.0–4.0

Table 2 Clusters of the significant correlations between the specific binding ratio (SBR) and gray matter volume

Anatomical region	Cluster size	Coordinates (mm)			
		x	y	z	Z score
Right posterior middle temporal gyrus	198	49.5	− 66.7	6.1	4.28
Right pulvinar	153	17.8	− 28.6	10.6	4.30
Left pulvinar	64	− 14.9	− 31.6	8.0	3.81

VBM analysis

The VBM analysis was performed using Christian Gaser's VBM toolbox (http://dbm.neuro.uni-jena.de/vbm8/) running within the Statistical Parametric Mapping software package ver. 8 (SPM8; http://www.fil.ion.ucl.ac.uk/spm). The gray matter probability values were then smoothed by using a 6-mm FWHM Gaussian kernel. The relationship between the gray matter volume and the SBR was assessed in a single linear correlation controlling for the patients' ages. Only differences that met these criteria were deemed significant. In this case, a seed level of $p < 0.001$ (uncorrected) and a cluster level of $p < 0.05$ (uncorrected) were used.

Results

The demographic and clinical characteristics of the PD patients are shown in Table 1. There were significant positive correlations in the right pulvinar (Fig. 1a) and the posterior middle temporal gyrus (Fig. 1b) and a trend level in the left pulvinar (Table 2) between the SBR and gray matter volume in the PD patients. There were no negative correlations between the SBR and gray matter volume in the PD patients. There were no significant correlations between the gray matter volume and clinical characteristics such as age, onset age, disease duration, L-dopa equivalent dose and Hoehn and Yahr scale.

Discussion

We investigated the relationship between gray matter volume and DAT density in PD patients. The 31 PD patients examined herein showed significant positive correlations between the SBR and gray matter volume in the right pulvinar and posterior middle temporal gyrus, both of which are responsible for a secondary visual pathway. To our knowledge, this
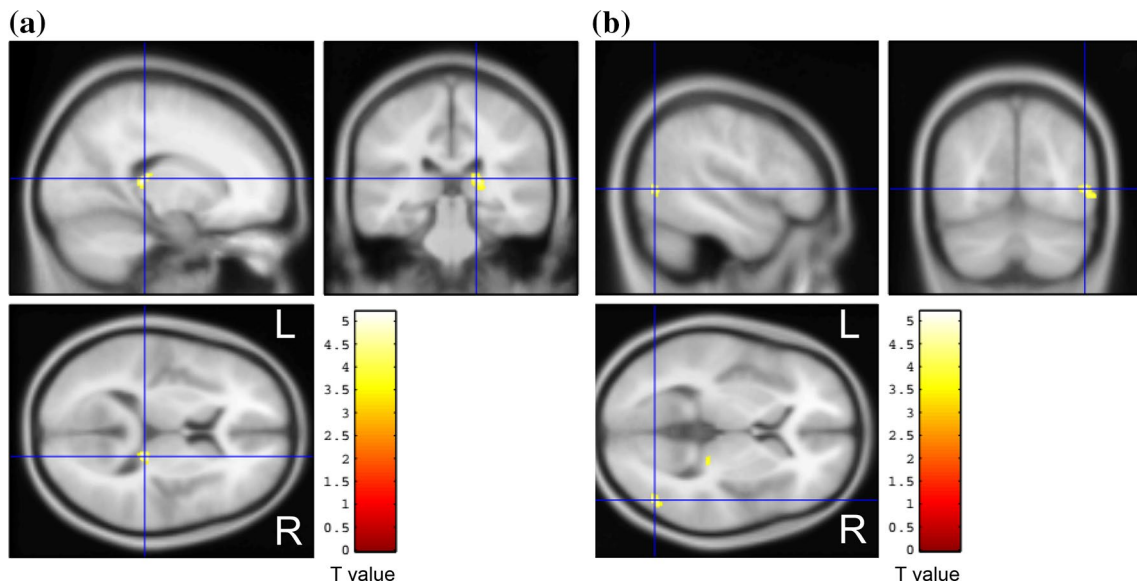

Fig. 1 Correlation between DAT binding and gray matter volume in PD patients. There were significant positive correlations between the SBR and gray matter volume in the right pulvinar (**a**) and posterior middle temporal gyrus (**b**). *L* left, *R* right

is the first study that evaluated the voxelwise correlation of gray matter volume with DAT density measured by DaTscan SPECT in PD patients.

The thalamus controls the processing of various types of information, and the pulvinar in particular plays a role as the gate of visual information [20]. Previous study indicates that pulvinar activities encode a subject's certainty of visual categorization and contribute to perceptual confidence [21]. A primary visual pathway consists of the optic nerve, the fibers of the optic nerve traveling through the optic chiasm to the lateral geniculate nucleus and optic radiations terminating in the primary visual cortex of an occipital lobe. There are two secondary visual pathways that do not pass through the primary visual cortex: the retino-colliculo-thalamo-amygdala pathway and the retino-geniculo-extrastriate pathway [22]. The former involves the thalamus, and it connects the retina through the superior colliculus and pulvinar to the extrastriate visual cortex, namely the motion area V5/medial temporal (MT) in the posterior middle temporal gyrus.

Diederich et al. proposed that aberrant function of these pathways underlies "the blind to blindsight syndrome" in PD patients [23]. This syndrome is the converse of blindsight, showing the erroneous 'guess' localization of visual stimuli, poor saccades and motion perception, and poor emotional face perception with blunted autonomic reaction. Visual hallucination is one of the common nonmotor symptoms of PD. In a functional MRI study in which healthy volunteers mimicked hallucinations by augmented reality technology, brain activations were seen in the amygdala, medial frontal cortex, occipito-temporal junction and thalamus [24].

Positron emission tomography (PET) with ^{18}F-fluorodeoxyglucose (^{18}F-FDG) showed that glucose consumption was reduced in occipito-temporal regions in PD patients with visual hallucinations compared to those without [25]. Moreover, it was reported that PD impaired the perception of motion, which is strongly linked with the motion area V5/MT [26, 27]. Though the mechanisms of visual dysfunctions including hallucinations in PD patients remain controversial, it seems possible that the pulvinar and posterior middle temporal gyrus may be associated with abnormal visual function in PD.

Only one study has evaluated the gray matter changes in association with nigrostriatal dopaminergic degeneration in PD patients by PET using ^{18}F-fluoropropyl-carbomethoxyiodophenylnortropane (^{18}F-FP-CIT) [23]; those authors (Choi et al. 2016) reported a trend for a positive correlation between the striatal binding ratio and gray matter volume in the cerebellum, parahippocampal gyrus and frontal cortex. Furthermore, they found a trend of negative correlation between the striatal binding ratio and gray matter density in the medial occipital cortex. Their results thus differ from ours. Though the cause of this difference is uncertain, several possibilities might explain this discrepancy. First, the difference is likely to be due to the different DAT imaging radioligands and modalities. Second, we calculated the SBR on the striatum, whereas Choi et al. calculated the SBR only on the putamen. Third, we analyzed only male patients, whereas Choi et al. analyzed both male and female. Further investigations by DaTscan SPECT, which is the most common DAT imaging technique, should be conducted.

Our study has several limitations. First, the subjects were limited to patients with PD; healthy controls were not included. Second, the sample size ($n = 31$) may not be large enough to draw a firm conclusion, and we analyzed only male patients. In fact, we could not find a significant correlation using family-wise error correction and a false discovery rate. Third, we analyzed using the minimum SBR between the left and right values. There was a trend level in the right pulvinar ($p = 0.057$) and the posterior middle temporal gyrus ($p = 0.056$). Furthermore, there were significant correlations only on the right side between the SBR and gray matter volume in the PD patients in this study. We think that the statistical significance would be clearer if our sample size were larger. Fourth, this was a cross-sectional study, and longitudinal randomized studies of larger populations are necessary to establish the true relationship between the gray matter volume and DAT density in PD patients. Fifth, the potential effects of antiparkinson drugs should be considered in future studies. Finally, the lack of clinical data about visual dysfunctions prohibits further pathophysiological evaluations related to the second visual pathway. More detailed clinical information including visual dysfunction should be examined in future studies.

Conclusions

We evaluated the relationship between gray matter volume changes and DAT density in PD patients using a VBM analysis. Positive correlations were found in the pulvinar and posterior middle temporal gyrus. Although we could not confirm visual dysfunctions of PD patients in our study, previous studies reported that the pulvinar and posterior middle temporal gyrus are associated with a secondary visual pathway. Our findings indicate a relationship between brain structural changes and DAT density, suggesting the involvement of the nigrostriatal dopaminergic degeneration in the pathophysiology of visual dysfunctions in PD. To clarify the conclusion, clinical visual information should be examined in future studies.

References

1. Jankovic J. Parkinson's disease: clinical features and diagnosis. J Neurol Neurosurg Psychiatry. 2008;79(4):368–76. doi:10.1136/jnnp.2007.131045.
2. Politis M. Neuroimaging in Parkinson disease: from research setting to clinical practice. Nat Rev Neurol. 2014;10(12):708–22. doi:10.1038/nrneurol.2014.205.
3. Suwijn SR, van Boheemen CJ, de Haan RJ, Tissingh G, Booij J, de Bie RM. The diagnostic accuracy of dopamine transporter SPECT imaging to detect nigrostriatal cell loss in patients with Parkinson's disease or clinically uncertain parkinsonism: a systematic review. EJNMMI Res. 2015;5:12. doi:10.1186/s13550-015-0087-1.
4. Cummings JL, Henchcliffe C, Schaier S, Simuni T, Waxman A, Kemp P. The role of dopaminergic imaging in patients with symptoms of dopaminergic system neurodegeneration. Brain. 2011;134(Pt 11):3146–66. doi:10.1093/brain/awr177.
5. Gerasimou G, Costa DC, Papanastasiou E, Bostanjiopoulou S, Arnaoutoglou M, Moralidis E, et al. SPECT study with I-123-ioflupane (DaTSCAN) in patients with essential tremor. Is there any correlation with Parkinson's disease? Ann Nucl Med. 2012;26(4):337–44. doi:10.1007/s12149-012-0577-4.
6. Burton EJ, McKeith IG, Burn DJ, Williams ED, O'Brien JT. Cerebral atrophy in Parkinson's disease with and without dementia: a comparison with Alzheimer's disease, dementia with Lewy bodies and controls. Brain. 2004;127(Pt 4):791–800.
7. Summerfield C, Junqué C, Tolosa E, Salgado-Pineda P, Gómez-Ansón B, Martí MJ, et al. Structural brain changes in Parkinson disease with dementia: a voxel-based morphometry study. Arch Neurol. 2005;62(2):281–5.
8. Beyer MK, Janvin CC, Larsen JP, Aarsland D. A magnetic resonance imaging study of patients with Parkinson's disease with mild cognitive impairment and dementia using voxel-based morphometry. J Neurol Neurosurg Psychiatr. 2007;78(3):254–9.
9. Melzer TR, Watts R, MacAskill MR, Pitcher TL, Livingston L, Keenan RJ, et al. Grey matter atrophy in cognitively impaired Parkinson's disease. J Neurol Neurosurg Psychiatr. 2012;83(2):188–94. doi:10.1136/jnnp-2011-300828.
10. Compta Y, Ibarretxe-Bilbao N, Pereira JB, Junqué C, Bargalló N, Tolosa E, et al. Grey matter volume correlates of cerebrospinal markers of Alzheimer-pathology in Parkinson's disease and related dementia. Parkinsonism Relat Disord. 2012;18(8):941–7. doi:10.1016/2012.04.028 (**j.parkreldis.**).
11. Sanchez-Castaneda C, Rene R, Ramirez-Ruiz B, Campdelacreu J, Gascon J, Falcon C, et al. Correlations between gray matter reductions and cognitive deficits in dementia with Lewy Bodies and Parkinson's disease with dementia. Mov Disord. 2009;24(12):1740–6. doi:10.1002/mds.22488.
12. Huang C, Mattis P, Tang C, Perrine K, Carbon M, Eidelberg D. Metabolic brain networks associated with cognitive function in Parkinson's disease. Neuroimage. 2007;34(2):714–23.
13. Huang C, Mattis P, Perrine K, Brown N, Dhawan V, Eidelberg D. Metabolic abnormalities associated with mild cognitive impairment in Parkinson disease. Neurology. 2008;70(16 Pt 2):1470–7.
14. Nobili F, Arnaldi D, Campus C, Ferrara M, De Carli F, Brugnolo A, et al. Brain perfusion correlates of cognitive and nigrostriatal functions in de novo Parkinson's disease. Eur J Nucl Med Mol Imaging. 2011;38(12):2209–18.
15. Choi H, Cheon GJ, Kim HJ, Choi SH, Kim YI, Kang KW, et al. Gray matter correlates of dopaminergic degeneration in Parkinson's Disease: a hybrid PET/MR study using (18) F-FP-CIT. Hum Brain Mapp. 2016;37(5):1710–21.
16. Hughes AJ, Daniel SE, Kilford L, Lees AJ. Accuracy of clinical diagnosis of idiopathic Parkinson's disease: a clinico-pathological study of 100 cases. J Neurol Neurosurg Psychiatr. 1992;55(3):181–4.
17. Hoehn MM, Yahr MD. Parkinsonism: onset, progression and mortality. Neurology. 1967;17(5):427–42.
18. Goetz CG, Poewe W, Rascol O, Sampaio C, Stebbins GT, Counsell C, et al. Movement Disorder Society Task Force report on the Hoehn and Yahr Staging scale: status and recommendations. Mov Disord. 2004;19(9):1020–8.
19. Tossici-Bolt L, Hoffmann SM, Kemp PM, Mehta RL, Fleming JS. Quantification of [123I]FP-CIT SPECT brain images: an accurate technique for measurement of the specific binding ratio. Eur J Nucl Med Mol Imaging. 2006;33(12):1491–9.
20. Robinson DL, Petersen SE. The pulvinar and visual salience. Trends Neurosci. 1992;15(4):127–32.
21. Komura Y, Nikkuni A, Hirashima N, Uetake T, Miyamoto A. Responses of pulvinar neurons reflect a subject's confidence in visual categorization. Nat Neurosci. 2013;16(6):749–55.
22. Danckert J, Rossetti Y. Blindsight in action: what can the different sub-types of blindsight tell us about the control of visually guided actions? Neurosci Biobehav Rev. 2005;29(7):1035–46.
23. Diederich NJ, Stebbins G, Schiltz C, Goetz CG. Are patients with Parkinson's disease blind to blindsight? Brain. 2014;137(Pt 6):1838–49. doi:10.1093/brain/awu094.
24. Ku J, Kim JJ, Jung YC, Park IH, Lee H, Han K, et al. Brain mechanisms involved in processing unreal perceptions. Neuroimage. 2008;43(4):793–800. doi:10.1016/j.neuroimage.2008.08.011.
25. Boecker H, Ceballos-Baumann AO, Volk D, Conrad B, Forstl H, Haussermann P. Metabolic alterations in patients with Parkinson disease and visual hallucinations. Arch Neurol. 2007;64(7):984–8.
26. Zeki S, Watson JD, Lueck CJ, Friston KJ, Kennard C, Frackowiak RS. A direct demonstration of functional specialization in human visual cortex. J Neurosci. 1991;11(3):641–9.
27. Tootell RB, Reppas JB, Kwong KK, Malach R, Born RT, Brady TJ, et al. Functional analysis of human MT and related visual cortical area using magnetic resonance imaging. J Neurosci. 1995;15(4):3215–30.